

## Theoretical Study on Rotation of Pyrrole Rings in Porphyrin and N-Confused Porphyrin

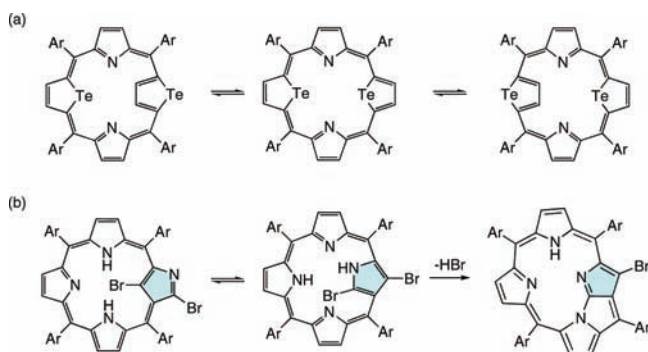
Motoki Toganoh and Hiroyuki Furuta\*

Department of Chemistry and Biochemistry, Graduate School of Engineering, Kyushu University, 744 Moto-oka, Nishi-ku, Fukuoka 819-0395, Japan

Received: June 30, 2009; Revised Manuscript Received: October 5, 2009

Rotation of pyrrole rings in regular porphyrins and N-confused porphyrins is theoretically investigated by DFT calculations. While the inversion of the pyrrole rings in the regular porphyrins requires high activation energies (36.5–49.1 kcal/mol), the inversion of the confused pyrrole rings in the N-confused porphyrins requires much lower activation energies (18.1–24.5 kcal/mol). This marked difference can be explained by the intramolecular hydrogen bondings and aromatic stabilization due to the [18]annulenic substructures, where confusion and NH tautomerism play an important role. In both of the macrocycles, 360° rotation of their pyrrole rings would be difficult possibly due to the small cavity. Alternatively, a reaction pathway for the production of N-fused porphyrin from N-confused porphyrin is obtained, which is consistent with the experimental observation.

## SCHEME 1: Rotation of the Pyrrole and Related Rings in Porphyrinoids



## 1. Introduction

Rotation is one of the most fundamental and important motions in molecular chemistry, which can, for example, be applicable to molecular machines.<sup>1</sup> Though many chemists have been fascinated with such motion, it is usually difficult to follow the consecutive conformational alteration, because taking snapshots of molecular rotation is hard to be achieved experimentally. Nevertheless, a theoretical approach gives critical information about rotational motion such as a rotational barrier of ethane.<sup>2</sup>

Rotation of pyrrole and related rings composing the main frameworks in porphyrin and related macrocycles often plays an important role, which results in the switching of electronic state, the construction of the unique architectures, and so on.<sup>3–5</sup> Whereas rotation of pyrrole rings is frequently observed in expanded porphyrins composed of five or more pyrrole rings, no experimental examples are reported in regular porphyrins composed of four pyrrole rings.<sup>6</sup> An exceptional example is the flipping of tellurophene rings in 21,23-ditelluraporphyrin (Scheme 1a).<sup>5</sup> The distinct difference between the regular porphyrins and the expanded porphyrins in pyrrole rotation can be explained by the strain and flexibility of the macrocyclic frameworks. The

tetrapyrrolic skeletons of the regular porphyrins usually take planar conformations and the strain in the [18]annulenic moieties is negligible. Besides, a facile formation of the intramolecular hydrogen bondings would strongly stabilize the planar conformations. Hence, higher energy should be required for the deformation of their rigid frameworks. On the other hand, the huge skeletons of the expanded porphyrins often take nonplanar conformations such as the figure of eight structures in octaphyrins to avoid a skeletal strain and have the high flexibility toward conformational alteration.<sup>7</sup>

N-Confused porphyrin, which is a pure isomer of porphyrin, has essentially the same rigid tetrapyrrolic framework as regular porphyrin.<sup>8</sup> However, rotation of the confused pyrrole ring occurs readily. For example, in the transformation of N-confused porphyrin into N-fused porphyrin, rotation of the confused pyrrole ring and subsequent C–N bond formation between the inverted confused pyrrole ring and the neighboring pyrrole ring would be essential (Scheme 1b).<sup>9–11</sup> Furthermore, the observation of an inverted conformer is possible by introduction of a bulky group into the inner carbon atom<sup>12</sup> or by metal coordination.<sup>13</sup> In solution, rotation of the confused pyrrole ring in N-confused porphyrin occurs even at room temperature, which shows a sharp contrast with rotation of the pyrrole ring in regular porphyrin where no experimental example has been reported.

This time, rotational motion of the pyrrole rings in regular porphyrins and N-confused porphyrins is theoretically investigated by density functional theory (DFT) calculations. Although the theoretical studies on the stability and structures of N-confused porphyrins and N-fused porphyrins including the NH tautomers as well as the pyrrole-inverted conformers were already reported in detail,<sup>14</sup> the energy barriers for pyrrole rotation have not been studied yet. Thus, calculations were performed on the transition state structures and the transient conformers for pyrrole rotation in the regular porphyrins and the N-confused porphyrins. In addition to the unsubstituted derivatives, the *meso*-aryl and  $\beta$ -alkyl substituted derivatives were also studied in detail. The regular porphyrins afforded the rotation pathway from the starting planar conformer to the inverted conformer with a high activation energy barrier (36.5–49.1 kcal/mol), while the N-confused porphyrins afforded

\* To whom correspondence should be addressed. E-mail: hfuruta@csf.kyushu-u.ac.jp.

the similar rotation pathway with a much lower activation energy barrier (18.1–24.5 kcal/mol). This marked difference can be rationalized by the intramolecular hydrogen bondings and aromatic stabilization, where confusion and NH tautomerism played an important role.<sup>15</sup> Besides, a reaction pathway from N-confused porphyrin to N-fused porphyrin is proposed in relation to the pyrrole rotation. Further rotation from an inverted conformer would readily give a fused structure like N-fused porphyrin in place of achieving a 360° rotation.

## 2. Computational Details

All density functional theory<sup>16</sup> calculations were achieved with a Gaussian03 program package.<sup>17</sup> The basis sets implemented in the program were used. The B3LYP density functional method<sup>18</sup> was used with the 6-31G\*\* basis set for structural optimizations, thermodynamic analyses, and IRC calculations, and the 6-311++G\*\* basis set was used for single point energies and NICS (nucleus-independent chemical shift) calculations.<sup>19</sup> The reliability of the calculations at the B3LYP/6-31G\*\* level is supported by the previous theoretical works on the porphyrin isomers.<sup>14</sup>

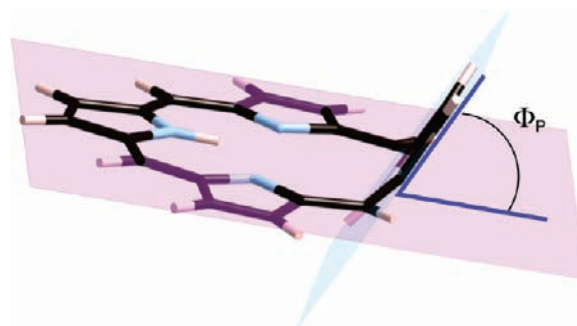
Equilibrium geometries were fully optimized and verified by the frequency calculations, where no imaginary frequency was found. Transition state geometries were also fully optimized and verified by the frequency calculations, where only one normal mode with an imaginary frequency was found. The character of the imaginary frequency was analyzed to confirm the presumable transition state for pyrrole rotation. IRC analyses were performed only on the unsubstituted derivatives for both sides of the transition states. Whereas the IRC calculations from the transition state structures often gave somewhat different structures from the equilibrium geometries obtained by the structural optimizations, further optimization from the IRC resulting structures always gave the expected equilibrium structures. The NICS values were calculated with the GIAO (gauge invariant atomic orbitals) method for the optimized structures.<sup>19</sup> All the NICS values were calculated at the center point of the 24 heavy atoms composing the porphyrin frameworks.

$E_R$  is relative energy in kcal/mol among conformers and  $E_A$  is an activation energy barrier in kcal/mol for pyrrole rotation at the B3LYP/6-311++G\*\*/B3LYP/6-31G\*\* level without the zero-point energy correction (denoted by  $\Delta H$ ). The corresponding Gibbs free energies under 1 atm at 298.15 K with the zero-point energy correction at the B3LYP/6-31G\*\* level are shown in the parentheses (denoted by  $\Delta G$ ). Because the effect of the zero-point energy correction as well as the thermodynamic factors on the relative energies is small and negligible, all the discussions below are based on  $\Delta H$ .

A rotational angle of pyrrole (denoted by  $\Phi_P$ ) is defined by the dihedral angle between the rotating pyrrole mean plane composed of 5 heavy atoms and the porphyrin mean plane composed of 19 heavy atoms of the porphyrin skeleton excluding the rotating pyrrole ring (Figure 1). A pyrrole ring bearing an NH moiety is called “amine-type pyrrole” and a pyrrole ring without a hydrogen atom on a nitrogen atom is called “imine-type pyrrole” (Chart 1). To distinguish porphyrin from N-confused porphyrin, it is called regular porphyrin in this manuscript.

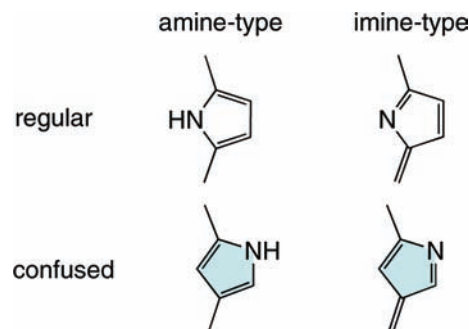
## 3. Results and Discussion

**3.1. Rotation of Pyrrole Ring in Porphyrin.** Calculations on unsubstituted porphyrin were performed and revealed that an amine-type pyrrole would rotate to give an inverted conformer via a presumable transition state with a high

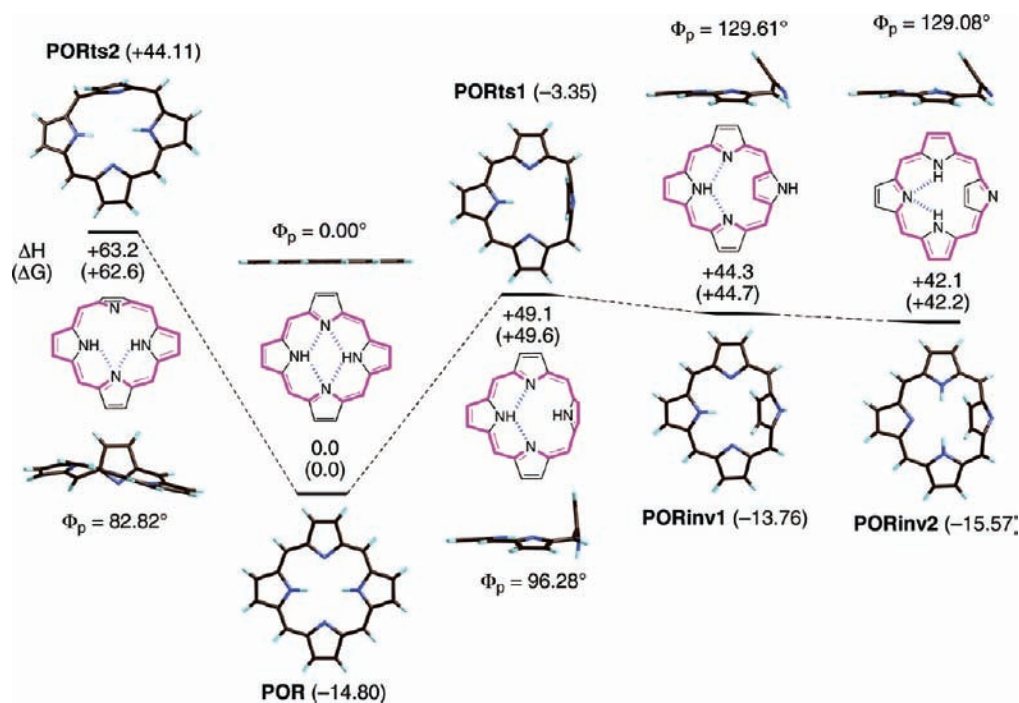


**Figure 1.** Conceptual diagram of  $\Phi_P$ .

### CHART 1: Category of Pyrrole Rings



activation energy barrier. The optimized structures and their relative energies are summarized in Scheme 2. Two pathways are considerable for pyrrole rotation from the most stable planar conformer (**POR**). One is the rotation of an amine-type pyrrole ring and another is the rotation of an imine-type pyrrole ring. For the rotation of the amine-type pyrrole ring, a reasonable transition state (**PORTs1**) was obtained. Meanwhile, no appropriate transition state has been found for the rotation of the imine-type pyrrole ring. The rotating amine-type pyrrole plane in **PORTs1** is nearly perpendicular to the porphyrin plane ( $\Phi_P = 96.3^\circ$ ). An activation energy barrier is fairly large ( $E_A = 49.1$  kcal/mol), which is consistent with the fact that no experimental example of pyrrole rotation is reported in regular porphyrins. Besides, an inverted conformer (**PORinv1**) is thermodynamically much less stable than the planar conformer, **POR** ( $E_R = +44.3$  kcal/mol). Therefore, it should be difficult to stabilize an inverted conformer experimentally in regular porphyrins even through the chemical modification such as installation of bulky groups inside a macrocycle. **PORinv2** has a similar shape ( $\Phi_P = 129.1^\circ$ ) and thermodynamic stability ( $E_R = +42.1$  kcal/mol) with its NH tautomer, **PORinv1** ( $\Phi_P = 129.6^\circ$ ). Figure 2 shows the relative energies and NICS values for the pyrrole rotation between **POR** and **PORinv1** through **PORTs1**. The values are changed smoothly during the pyrrole rotation, which supports that the structures of **POR**, **PORTs1**, and **PORinv1** calculated here would be reasonable. Though no appropriate transition state for the rotation of the imine-type pyrrole ring has been found, an alternative transition state (**PORTs2**), which is much less stable than the other conformers ( $E_R = +63.2$  kcal/mol), was obtained. Whereas the rotating pyrrole plane is nearly perpendicular to the porphyrin plane ( $\Phi_P = 82.8^\circ$ ), like **PORTs1**, the porphyrin framework is waved significantly. Note that the tripyrrane unit in **PORTs1** is nearly planar. In the IRC analysis, a reaction pathway between **POR** and **PORTs2** is found, but no pathway from **PORTs2** to **PORinv2** has been found. In turn, dissociation of a C–H bond at a *meso*-position is observed. This pathway is consistent with the character of the normal mode with an imaginary frequency in **PORTs2**.

SCHEME 2: Energy Profile for the Rotation of Pyrrole Rings in the Regular Porphyrin<sup>a</sup>

<sup>a</sup> The relative energies ( $\Delta H$  and  $\Delta G$ ) are reported in kcal/mol, and the NICS values in ppm are described in the parentheses next to the abbreviated name. The dotted lines indicate the intramolecular hydrogen bonds.

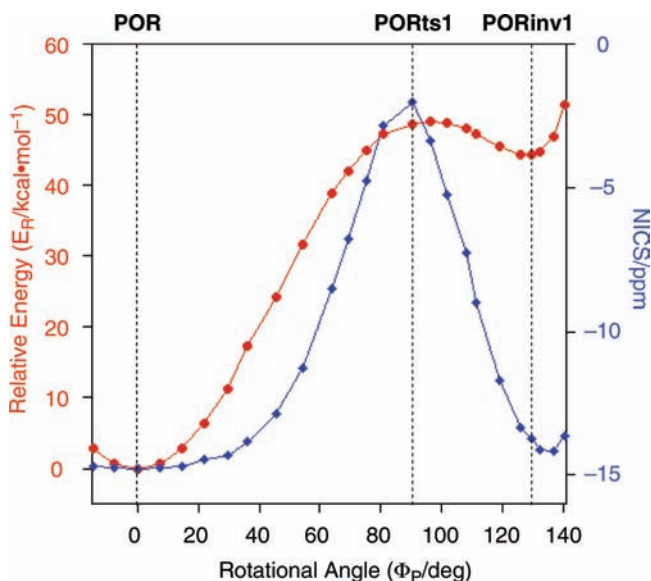


**Figure 2.** Relative energies and NICS values for the pyrrole rotation between **POR** and **PORinv1** through **PORTs1**.

A correlative relationship between the energy profile and aromaticity is discussed on the basis of the NICS values (Scheme 2) and the Kohn–Sham orbitals (Figures 3 and 4). **POR** has a large negative NICS value ( $-14.80$  ppm), suggesting strong aromaticity due to the planar [18]annulenic substructure. Although the conformations in the inverted conformers (**PORinv1** and **PORinv2**) are far from planar, they still have strongly negative NICS values ( $-13.76$  and  $-15.57$  ppm, respectively). The Kohn–Sham orbitals of **PORinv1** are essentially same as those of **POR** without the conformation of the [18]annulenic skeleton (Figures 3a–f).<sup>20</sup> Namely, by rotating the amine-type pyrrole in the HOMO and LUMO of **POR**, those of **PORinv1** can be constructed. Thus, the instability of the inverted conformers would not derive from electronic natures, but from

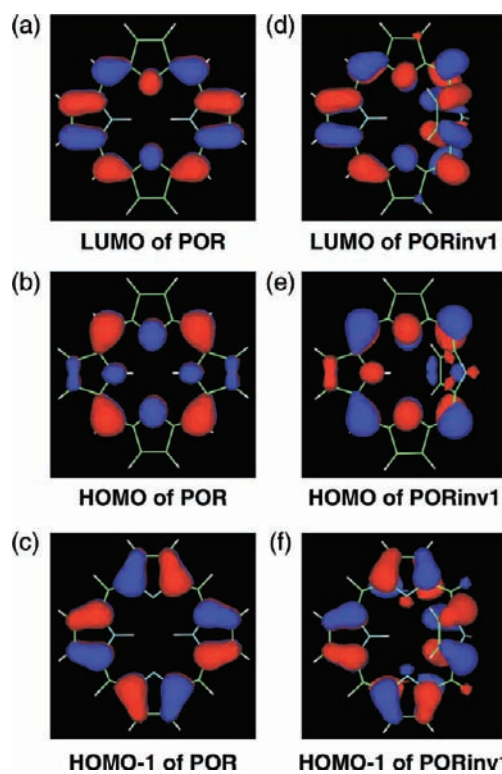


**Figure 3.** Kohn–Sham orbitals of (a–c) **POR** and (d–f) **PORinv1**.

the strain imposed by the distorted [18]annulenic skeletons. In **PORTs1**, a small negative NICS value ( $-3.35$  ppm) is obtained, which suggests a nearly nonaromatic character of **PORTs1**. Because the rotating pyrrole plane is almost perpendicular to the porphyrin plane ( $\Phi_p = 96.3^\circ$ ), no effective orbital overlapping between the rotating pyrrole ring and the rest tripyrrane unit is expected. Actually, the occupied orbital of the rotating pyrrole moiety (HOMO-1) and that of the rest tripyrrane moiety



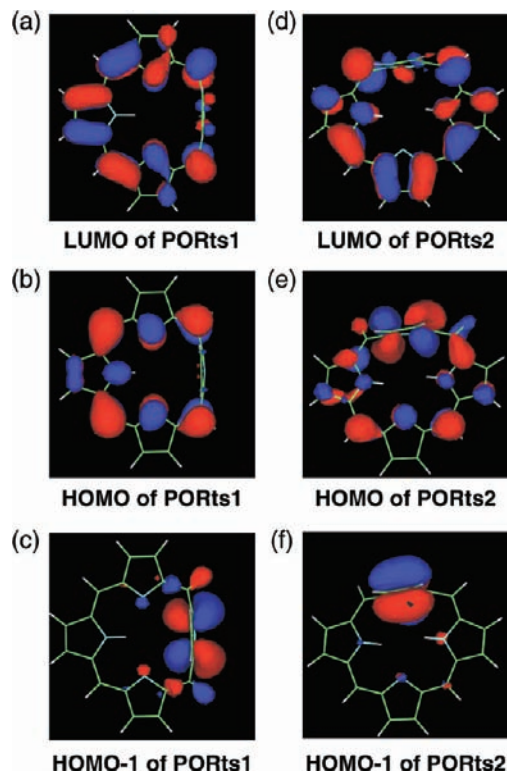


Figure 4. Kohn-Sham orbitals of (a–c) **PORTs1** and (d–f) **PORTs2**.

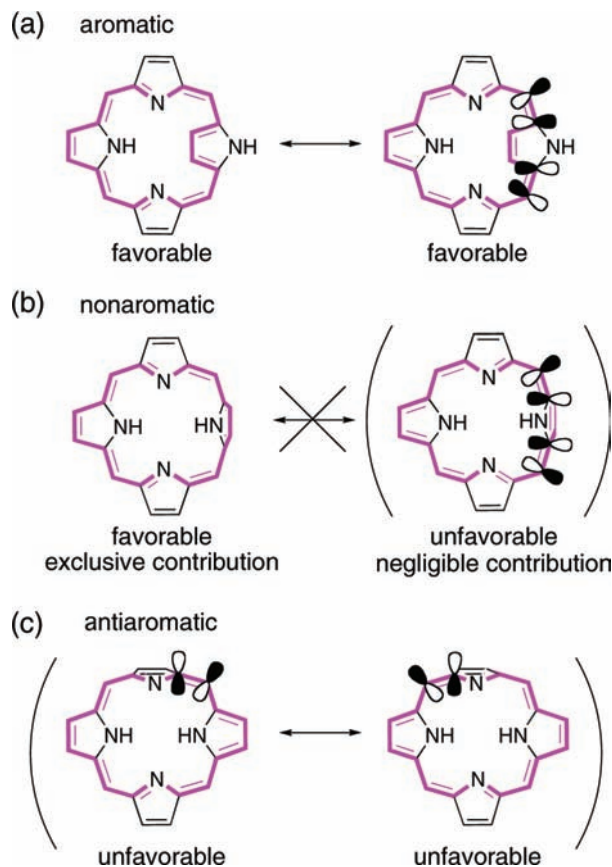
(HOMO) are separately observed as shown in Figure 4b,c unlike **PORinv1** (Figure 3e,f). Interestingly, **PORTs2** gives an unusually large positive NICS value (+44.11 ppm). This might be explained by Möbius antiaromaticity of [18]annulenes.<sup>21–23</sup> In the HOMO of **PORTs2**, a contribution of both of the rotating pyrrole moiety and the rest tripyrrane moiety is distinctly observed in spite of the nearly perpendicular conformation ( $\Phi_P = 82.8^\circ$ ). This conflict can be resolved by a Möbius-type phase inversion shown in Figure 4e.

The discussion described above is in line with the classical Kekulé description of [18]annulenes. For example, a pair of the favorable resonance structures possessing the [18]annulenic  $\pi$ -circuit can be described for **POR**, **PORinv1**, and **PORinv2**, all of which show the strong aromatic characters (Scheme 3a). In **PORTs1**, the carbon–carbon bonds between the rotating pyrrole ring and the neighboring *meso*-carbon atoms prefer a single bond, because the geometry around these bonds is far from planar. Retention of a double bond character at this part, namely, existence of the twisted carbon–carbon double bond, would be thermodynamically unfavorable and, thus, only one of the two resonance Kekulé structures contributes in **PORTs1** (Scheme 3b). It suggests a loss of aromaticity in **PORTs1** and actually the NICS value indicates the nonaromatic character of **PORTs1** (–3.35 ppm). Contrastingly, in **PORTs2**, while the two resonance Kekulé structures can be described, one of the two carbon–carbon bonds connecting the rotating pyrrole ring and the rest tripyrrane moiety should possess a double bond character in both of the Kekulé structures (Scheme 3c). Hence, it is inevitable to have the twisted double bond within its [18]annulenic substructure, resulting in strong antiaromaticity (NICS: +44.11 ppm) and less stability.

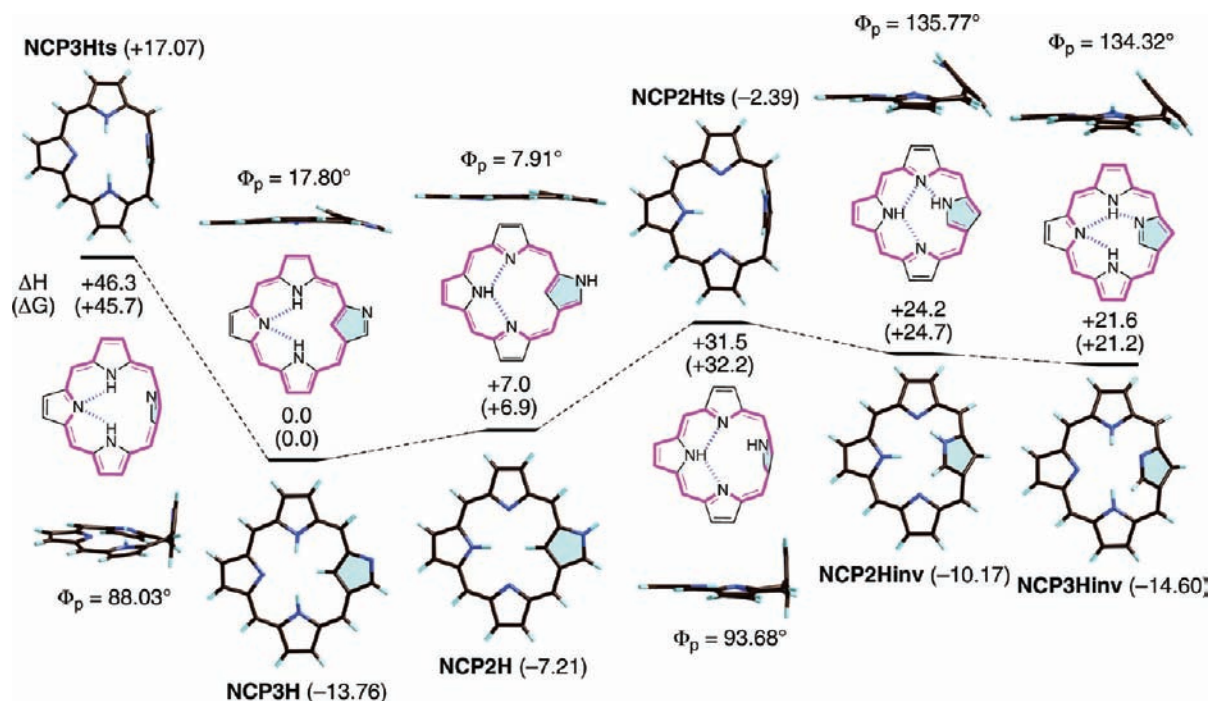
### 3.2. Rotation of Pyrrole Ring in N-Confused Porphyrin.

Next, calculations on N-confused porphyrin frameworks were performed to reveal why the confused pyrrole rings rotate readily (Scheme 4). Because the four nitrogen atoms are nonequivalent,

SCHEME 3: Resonance Structures of (a) **PORinv1**, (b) **PORTs1**, and (c) **PORTs2**

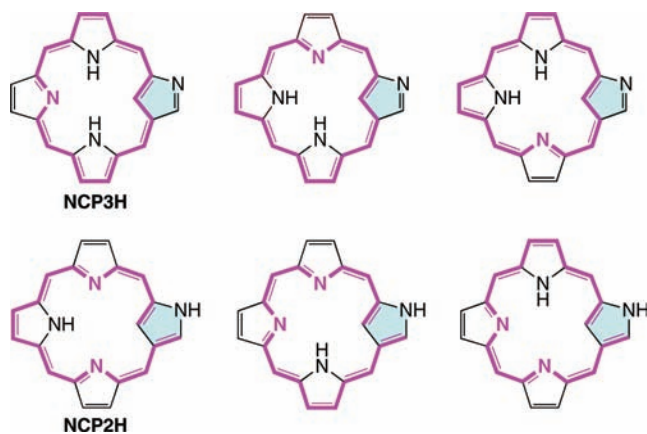


there exist six NH tautomers in N-confused porphyrin (Chart 2). Among them, the two important tautomers, **NCP3H** ( $E_R = 0.0$  kcal/mol) and **NCP2H** ( $E_R = +7.0$  kcal/mol), were subjected to the calculations. In a similar manner to the regular porphyrin, an appropriate transition state is only found for the rotation of an amine-type pyrrole ring (**NCP2Hts**), where the confused pyrrole ring is almost perpendicular to the porphyrin plane ( $\Phi_P = 93.68^\circ$ ) similar to **PORTs**. As shown in Figure 5, both of the relative energies and NICS values are changed smoothly during the pyrrole rotation from **NCP2H** to **NCP2Hinv** via **NCP2Hts**, which reasonably supports the reasonability of the calculation result. No appropriate transition state is obtained for the rotation of an imine-type pyrrole ring. An alternative transition state (**NCP3Hts**), which is not a transition state for the pyrrole rotation, was found. It has a similar character to **PORTs2** such as a high activation energy barrier (+46.3 kcal/mol) and an antiaromatic twisted structure ( $\Phi_P = 88.0^\circ$ , NICS = +17.07 ppm). These results mean that the rotation of the confused pyrrole starts not from **NCP3H** but from **NCP2H**. Intriguingly, the confused pyrrole ring in **NCP2H** is connected to the rest of the tripyrrane unit with two carbon–carbon single bonds in the classical Kekulé description, which would be the proper arrangement for the pyrrole rotation. An activation energy barrier for the confused pyrrole rotation is only 24.5 kcal/mol, which is much lower than that of the unsubstituted regular porphyrin (49.1 kcal/mol). In the inverted conformers, **NCP2Hinv** ( $E_R = +24.2$  kcal/mol) and **NCP3Hinv** ( $E_R = +21.6$  kcal/mol), the energy difference from the stable conformers, **NCP2H** and **NCP3H**, are much smaller (17.2 and 21.6 kcal/mol, respectively) than that of the regular porphyrin (44.3 and 42.1 kcal/mol), which can be explained by the formation of the intramolecular hydrogen bonding between the confused pyrrole ring

SCHEME 4: Energy Profile for the Rotation of Confused Pyrrole Rings in the N-Confused Porphyrin<sup>a</sup>

<sup>a</sup> The relative energies ( $\Delta H$  and  $\Delta G$ ) are reported in kcal/mol, and the NICS values in ppm are described in the parentheses next to the abbreviated name. The dotted lines indicate the intramolecular hydrogen bondings.

## CHART 2: NH Tautomers of N-Confused Porphyrin



and the neighboring pyrrole ring in the inverted conformers (vide infra). Rotational angles of the confused pyrrole ( $\Phi_P = 135.8^\circ$  for **NCP2Hinv**,  $\Phi_P = 134.3^\circ$  for **NCP3Hinv**) are slightly larger than those of the regular pyrrole in **PORinv1** ( $\Phi_P = 129.6^\circ$ ) and **PORinv2** ( $\Phi_P = 129.1^\circ$ ). It would support the stabilization by the intramolecular hydrogen bondings inside the macrocycles in **NCP2Hinv** and **NCP3Hinv**.

The geometric features of the Kohn–Sham orbitals for the N-confused porphyrin framework closely resemble those for the regular porphyrin framework (Figures 6–8). In both the planar and inverted conformations, no significant differences are found between the inner 2H-type tautomers (**NCP2H** and **NCP2Hinv**, Figure 6) and the inner 3H-type tautomers (**NCP3H** and **NCP3Hinv**, Figure 7), all of which share the same features as **POR** and **PORinv1**. The orbitals of **NCP2Hts** resemble those of **PORts1** and support its nonaromatic character (Figure 8a–c). For example, the orbital of the confused pyrrole ring and the orbital of the rest tripyrrane moiety are separately observed in the HOMO-1 (Figure 8c) and the HOMO (Figure 8b), respectively. In a similar fashion, the orbitals of **NCP3Hts** resemble

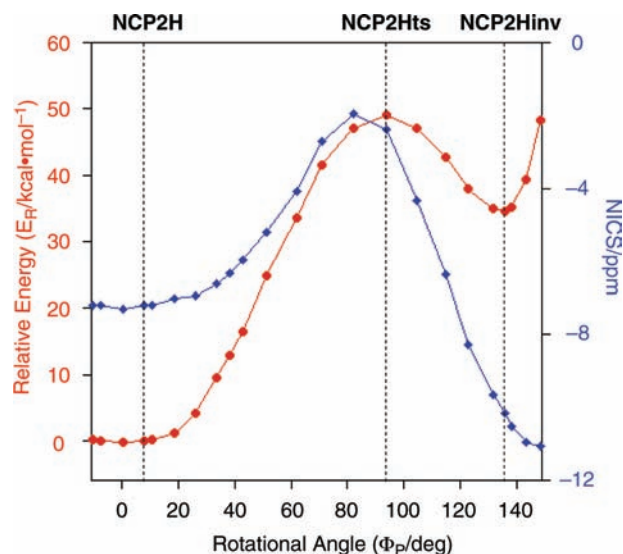


**Figure 5.** Relative energies and NICS values for the confused pyrrole rotation between **NCP2H** and **NCP2Hinv** through **NCP2Hts**.

those of **PORts2** and support its antiaromatic character, which can be rationalized by the Möbius-ring-type orbital overlapping (Figure 8d–f).

To validate the utility of confused-linkage, the rotation of the other pyrrole rings in N-confused porphyrin was examined (Scheme 5). Evidently, the rotation of the confused pyrrole gives the smallest activation energy barrier ( $E_A = 24.5$  kcal/mol) and the rotation of the regular pyrrole rings requires much larger activation energies ( $E_A = 37.4$ – $58.2$  kcal/mol). The rotation of the regular pyrrole rings is usually accompanied by cleavage of the intramolecular hydrogen bondings inside the macrocycle, which would cause a higher activation energy barrier. Meanwhile, the confused pyrrole already loses the intramolecular hydrogen bondings and is ready to rotate. All the transition state structures have slightly negative NICS values ( $-2.39$ – $-4.61$



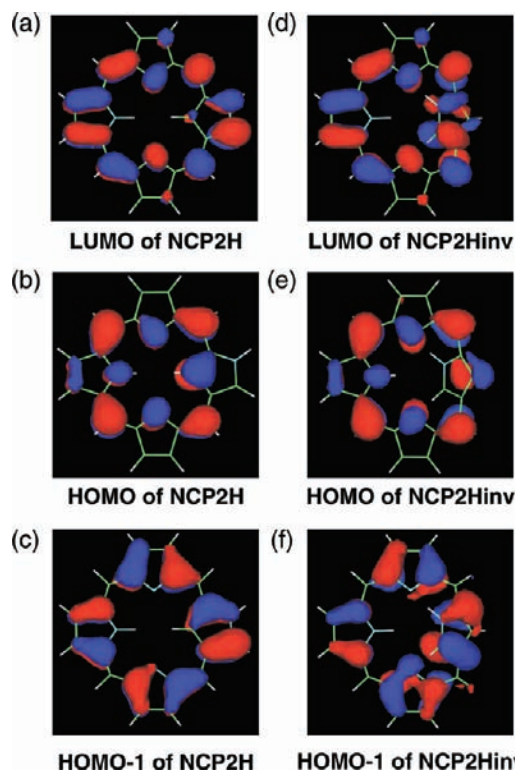


Figure 6. Kohn-Sham orbitals of (a–c) NCP2H and (d–f) NCP2Hinv.

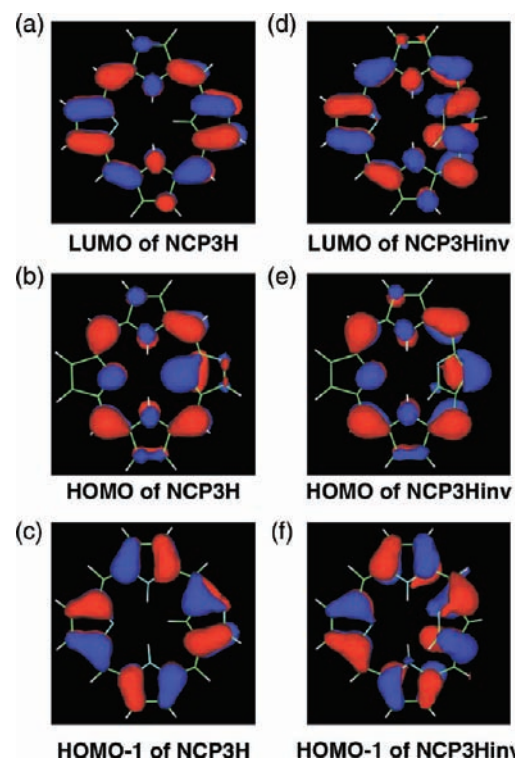


Figure 7. Kohn-Sham orbitals of NCP3H and NCP3Hinv.

ppm) and, consequently, the aromatic stabilization cannot account for the difference in the activation energy barriers.

**3.3. Comparison of Regular Porphyrin and N-Confused Porphyrin in Pyrrole Rotation.** The origin of the much lower activation energy barrier in the N-confused porphyrin than that in the regular porphyrin is discussed based on the intramolecular hydrogen bondings, aromatic stabilization, and steric factor. The relative energies for the pyrrole rotation in the regular porphyrin

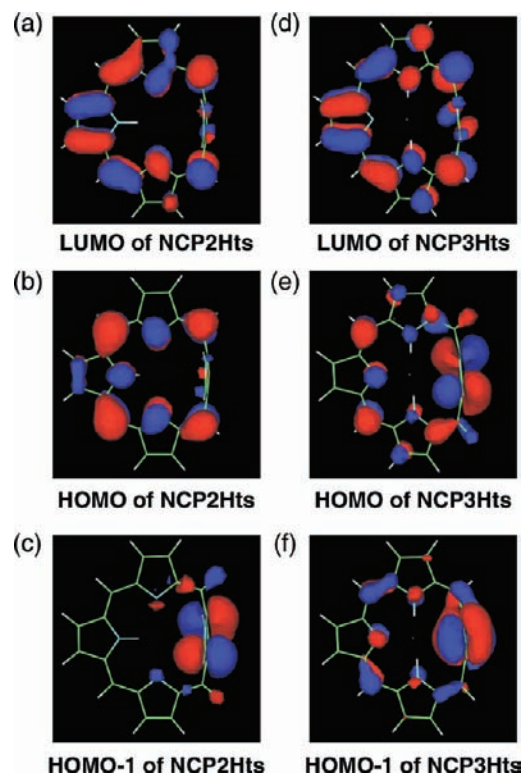
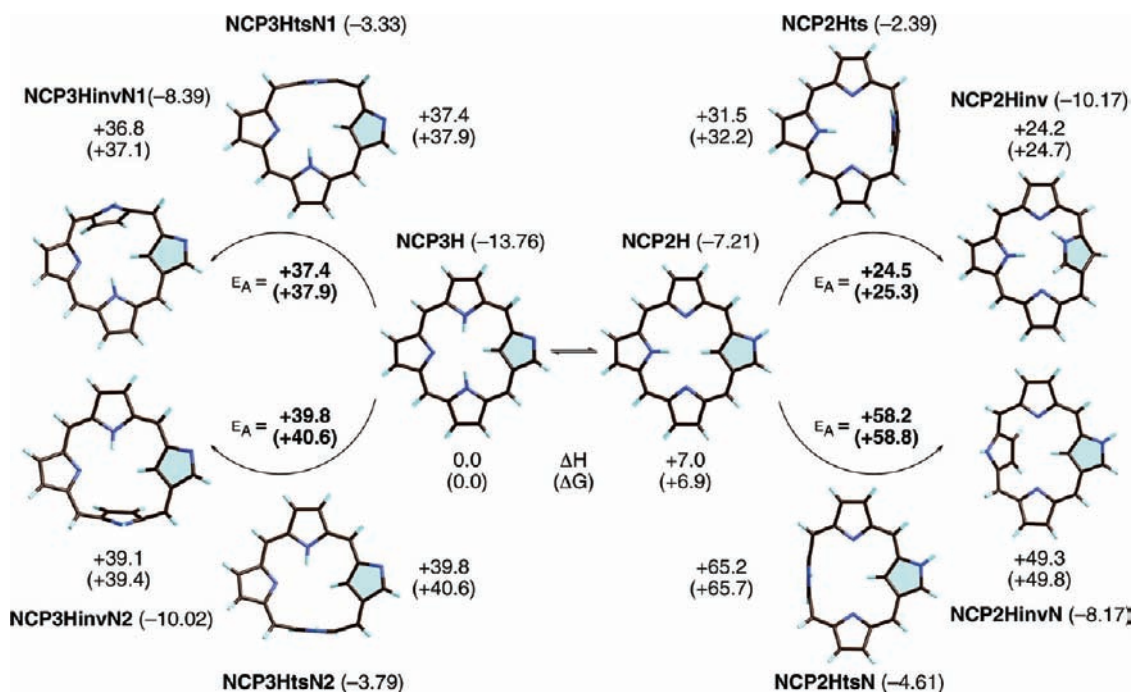


Figure 8. Kohn-Sham orbitals of NCP2Hts and NCP3Hts.

framework and the N-confused porphyrin framework are summarized in Figure 9.

**3.3.1. Transition State.** Interestingly, **PORTs1** and **NCP2Hts** have almost the same energy. In both of the transition state structures, the rotating pyrrole ring and the rest tripyrrane unit are perpendicular to each other and then the orbital interaction between two moieties is not effective as discussed above. Accordingly, **PORTs1** (NICS =  $-3.35$  ppm) and **NCP2Hts** (NICS =  $-2.39$  ppm) exhibit nearly the nonaromatic character. The intramolecular N-NH-N hydrogen bondings in the tripyrrane unit would be similar to each other in **PORTs1** and **NCP2Hts**, because the structures of the tripyrrane moieties are nearly identical (Figure 10). Besides, the ring strain or steric repulsion should also be similar to each other in **PORTs1** and **NCP2Hts** because of the same reason. In essence, the confusion effect is negated in the transition state and, thus, **PORTs1** and **NCP2Hts** share the same features. Thus, the consideration to the transition states could not account for the difference in the activation energy barrier.

**3.3.2. Initial State.** Because **PORTs1** and **NCP2Hts** have almost the same thermodynamic stability, the difference in the activation energy barriers in the regular porphyrin and the N-confused porphyrin is derived from the difference of the thermodynamic stability in the initial states, **POR** and **NCP2H**. Namely, analysis of the factors to destabilize **NCP2H** over **POR** is critically important in this study. Both of the initial states are almost planar ( $\Phi_P = 0.00^\circ$  for **POR** and  $7.91^\circ$  for **NCP2H**) and have the similar geometries (Figure 11). Then the ring strain or steric repulsion would be a less important factor. A small deviation from planarity in **NCP2H** might contribute to decrease the activation energy barrier, but this effect would be very weak or negligible. Because the relative energies were not so changed between  $\Phi_P = 0^\circ$  and  $\Phi_P = 20^\circ$  in Figures 2 and 5. Meanwhile, a partial loss of aromatic stabilization in **NCP2H** would play a significant role in the lower activation energy barrier. **POR** is strongly aromatic (NICS =  $-14.80$  ppm) and stabilized due to

SCHEME 5: Energy Profile for the Rotation of Pyrrole Rings in the N-Confused Porphyrin<sup>a</sup>

<sup>a</sup> The relative energies ( $\Delta H$  and  $\Delta G$ ) are reported in kcal/mol, and the NICS values in ppm are described in the parentheses next to the abbreviated name.

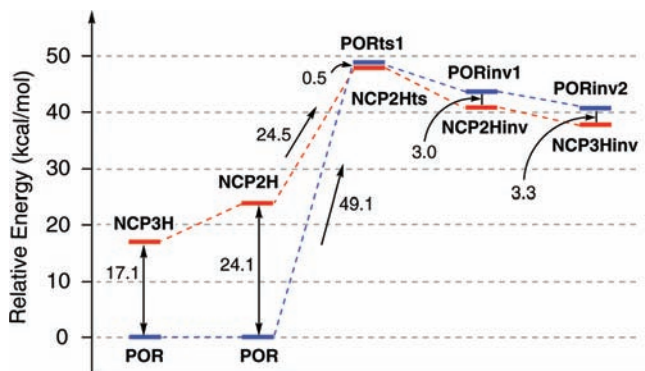


**Figure 9.** Energy profile for the pyrrole rotation in the regular porphyrin and the N-confused porphyrin.

the [18]annulenic substructure. In contrast, **NCP2H** is moderately aromatic (NICS =  $-7.21$  ppm), because a complete [18]annulenic circuit cannot be described unlike **POR** and **NCP3H** (NICS =  $-13.76$  ppm). Eventually, NH tautomerization from **NCP3H** to **NCP2H** causes a partial loss of aromatic stabilization, which results in the less stability of **NCP2H** and, consequently, the lower activation energy barrier for the pyrrole rotation in the N-confused porphyrin. Although it is difficult to estimate the degree of destabilization solely due to the partial loss of aromaticity, it is estimated roughly to be 5–10 kcal/mol on the basis of the energy difference between **NCP2H** and **NCP3H**. Finally and most importantly, a loss of intramolecular hydrogen bondings inside the macrocycle should be a definite factor to destabilize **NCP2H**. In the case of **POR**, the circular N-NH-N-NH hydrogen bondings are expected inside the macrocycle, which would strongly stabilize the planar conformation. Only the noncircular N-NH-N hydrogen bondings are possible in **NCP2H**, and the stabilization of the planar conformation with this noncircular interaction would be much weaker than with the circular interaction. On the assumption that the energy difference between **NCP2H** and **POR** (24.1 kcal/mol) is

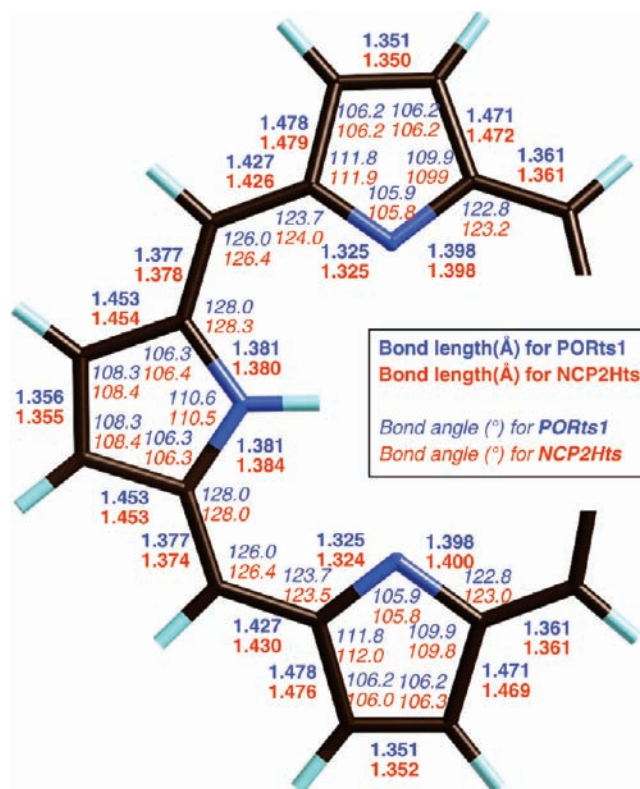
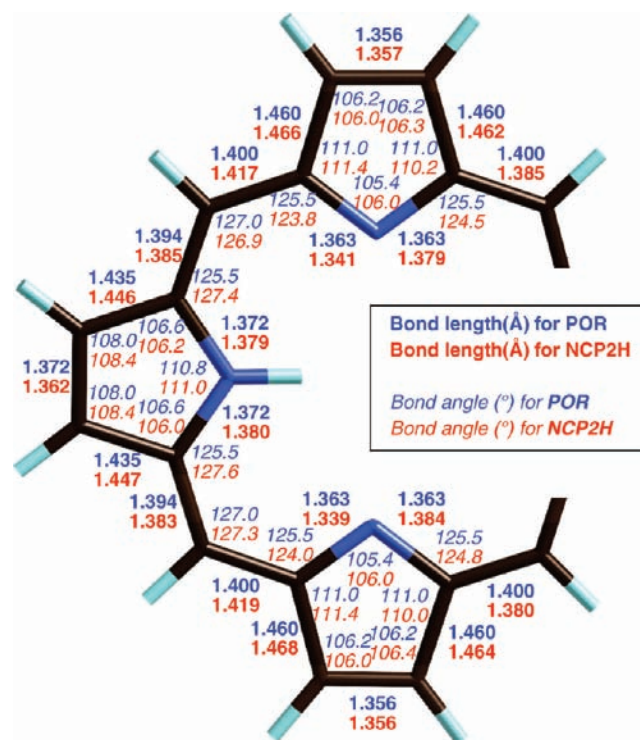


**Figure 10.** Bond lengths and angles of the tripyrrane moieties in **PORts1** and **NCP2Hts**.

explained reasonably by the intramolecular hydrogen bondings and the aromatic stabilization (5–10 kcal/mol), a loss of hydrogen binding in **NCP2H** compared to **POR** would cause destabilization in 15–20 kcal/mol.

**3.3.3. Inverted State.** Although the regular porphyrin is much more stable than the N-confused porphyrin when they take the planar conformation, the N-confused porphyrin (**NCP2Hinv** and

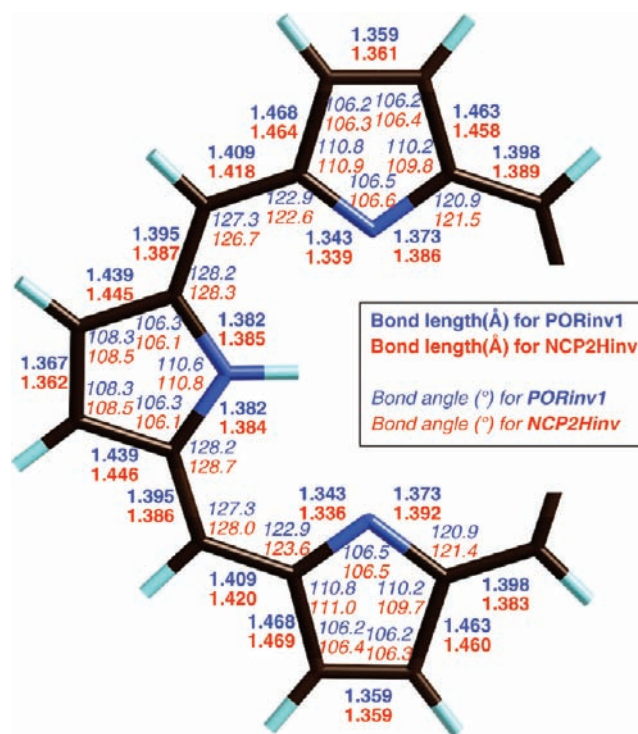




**Figure 11.** Bond lengths and angles of the tripyrrane moieties in **POR** and **NCP2H**.

**NCP3Hinv**) becomes more stable than the regular porphyrin (**PORinv1** and **PORinv2**) by about 3 kcal/mol in the inverted conformation. This reversal of the relative stability between the regular porphyrin and the N-confused porphyrin can be explained also by the intramolecular hydrogen bondings. In the inverted conformation, the porphyrin frameworks should be highly strained and destabilized compared to those in the planar conformation. Nevertheless, the geometries of **NCP2Hinv** and **PORinv1** are still similar to each other (Figure 12) and then the degree of the destabilization due to the ring strain would also be similar between **NCP2Hinv** and **PORinv1**. The marked difference between **NCP2Hinv** and **PORinv1** is the position of the NH moiety on the inverted pyrrole ring. In **PORinv1**, two CH moieties of the inverted pyrrole ring are placed inside the macrocycle and no hydrogen bondings are expected. On the other hand, one CH moiety and one NH moiety are placed inside in **NCP2Hinv**, where a formation of hydrogen bonding with the neighboring imine-type pyrrole ring can be expected though the geometry is not so advantageous for the hydrogen binding. The NICS values indicate that both **PORinv1** and **NCP2Hinv** are strongly aromatic, in which the former is stronger. From the viewpoint of aromatic stabilization, **PORinv1** is favorable. In summary, **NCP2Hinv** is favorable for the hydrogen bondings and unfavorable for the aromatic stabilization. Here the influence of the hydrogen bondings would be stronger and then **NCP2Hinv** is slightly more stable than **PORinv1**. The energy difference between **PORinv2** and **NCP3H** can be explained in the same way.

**3.4. Formation of N-Fused Porphyrin from N-Confused Porphyrin.** In the tetrapyrrolic skeletons, the 360° rotation of the pyrrole ring would be difficult because of the small cavity inside the macrocycles. The attempted optimization for a transition state with  $\Phi_p \sim 180^\circ$  did not afford any suitable structures for a 360° rotation so far. Instead, a reaction pathway for the intramolecular C–N bond formation was found in the calculation on the N-confused porphyrin, which is consistent

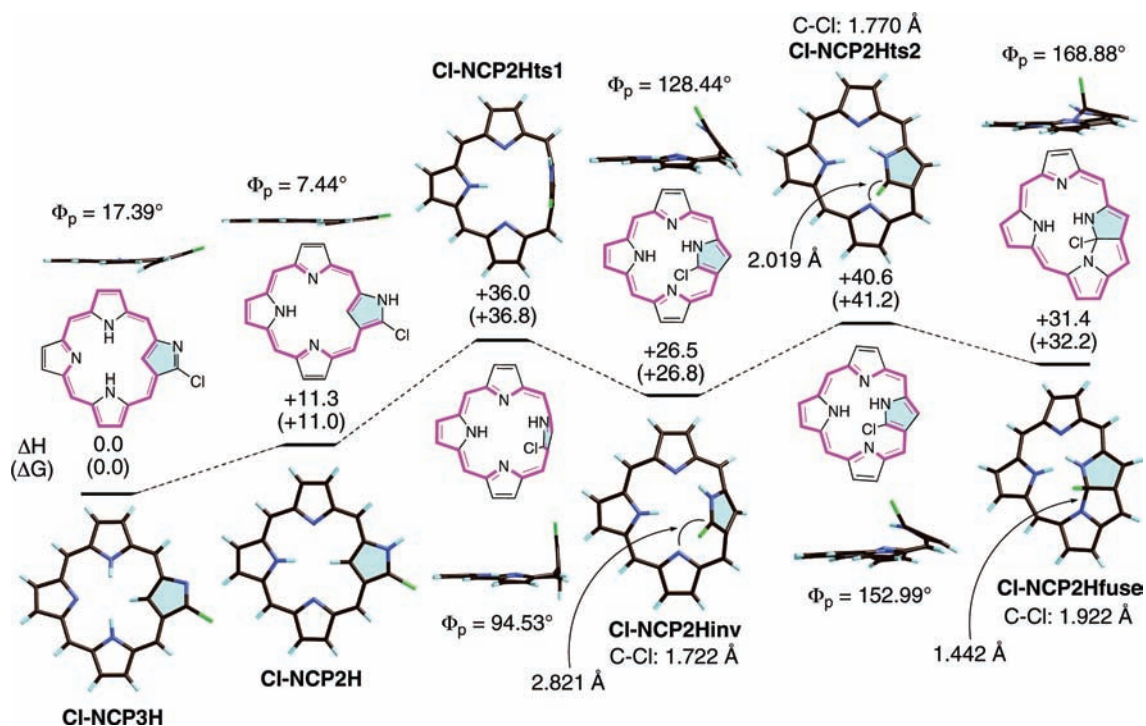


**Figure 12.** Bond lengths and angles of the tripyrrane moieties in **PORinv1** and **NCP2Hinv**.

with the formation of N-fused porphyrin from N-confused porphyrin.<sup>9,10</sup> In Scheme 6, the calculation results on the rotation of the confused pyrrole ring in the chlorinated N-confused porphyrin are shown, which afford a plausible mechanism for the formation of the N-fused porphyrin.<sup>24</sup> The rotation from **Cl-NCP2H** to **Cl-NCP2Hinv** requires almost the same activation energy ( $E_A = 24.7$  kcal/mol) as the unsubstituted case ( $E_A = 24.5$  kcal/mol). The trial of a further rotation from **Cl-NCP2Hinv** causes the approximation of the  $\alpha$ -carbon atom in the confused pyrrole ring to the nitrogen atom in the adjacent pyrrole ring. In **Cl-NCP2Hinv**, the C–N distance is 2.821 Å and it becomes 2.019 Å in the transition state (**Cl-NCP2Hts2**). Then the C–N bond (1.442 Å) is definitely formed in **Cl-NCP2Hfuse**. Accordingly, the C–Cl bond increases in length from 1.722 to 1.922 Å. The activation energy barrier for the C–N bond formation is rather small (14.1 kcal/mol), and then this step would proceed readily. Finally, a loss of an HCl molecule from **Cl-NCP2Hfuse** causes the production of the N-fused porphyrin. Although **Cl-NCP2Hfuse** could readily go back to **Cl-NCP2Hinv** and then to **Cl-NCP2H** because of its instability, the loss of the HCl molecule should be a good driving force for the facile production of the N-fused porphyrin. Actually, the formation of N-fused porphyrin from halogenated N-confused porphyrin is largely accelerated in a pyridine solution.<sup>9</sup>

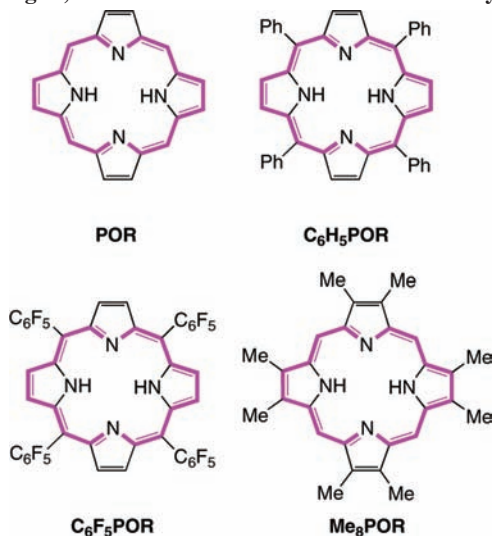
**3.5. Substitution Effect.** Finally, the substituent effects at the *meso*- as well as the pyrrolic  $\beta$ -positions were investigated. The calculations were performed on the *meso*-phenyl, *meso*-pentafluorophenyl, and  $\beta$ -methyl derivatives for both of the regular and N-confused porphyrins, and the results are listed in Tables 1 and 2, respectively. Introduction of the *meso*-phenyl groups to **POR** causes the considerable decrease of an activation energy barrier ( $E_A = 36.5$  kcal/mol for **C<sub>6</sub>H<sub>5</sub>POR** and 49.1 kcal/mol for **POR**). Because no significant differences in the structures of the porphyrin frameworks as well as the NICS values are found, the decrease of the activation energy barrier by 13 kcal/mol would be mainly explained by the steric



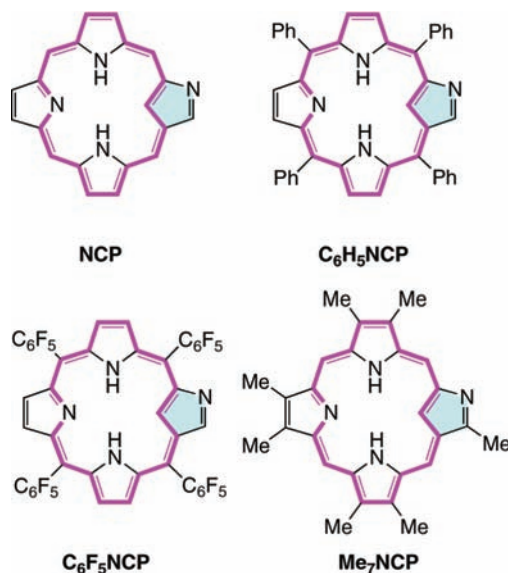
SCHEME 6: Energy Profile for the Rotation of Pyrrole Rings in the Chlorinated N-Confused Porphyrin<sup>a</sup>

<sup>a</sup> The relative energies ( $\Delta H$  and  $\Delta G$ ) are reported in kcal/mol. Selected interatomic distances are also shown.

TABLE 1: Energy Profiles, Rotational Angles, and NICS Values for the Rotation of Pyrrole Rings in the Regular Porphyrins



	$E_A$ (kcal/mol)		POR	PORts1	PORinv1	PORinv2
<b>POR</b>	$\Delta H$ 49.1	$E_R$ (kcal/mol)	0.0	+49.1	+44.3	+42.1
	$(\Delta G$ 49.6)	$\Delta H$ ( $\Delta G$ )	(0.0)	(+49.6)	(+44.7)	(+42.2)
		$\Phi_p$ (deg)	0.0	96.3	129.6	129.1
		NICS (ppm)	-14.80	-3.35	-13.76	-15.57
<b>C<sub>6</sub>H<sub>5</sub>POR</b>	$\Delta H$ 36.5	$E_R$ (kcal/mol)	0.0	+36.5	+29.0	+28.7
	$(\Delta G$ 36.7)	$\Delta H$ ( $\Delta G$ )	(0.0)	(+36.7)	(+29.7)	(+28.8)
		$\Phi_p$ (deg)	6.0	87.3	129.9	130.5
		NICS (ppm)	-13.69	-1.68	-11.56	-12.82
<b>C<sub>6</sub>F<sub>5</sub>POR</b>	$\Delta H$ 40.4	$E_R$ (kcal/mol)	0.0	+40.4	+33.6	+31.8
	$(\Delta G$ 38.8)	$\Delta H$ ( $\Delta G$ )	(0.0)	(+38.8)	(+32.2)	(+30.6)
		$\Phi_p$ (deg)	4.3	94.2	130.4	130.2
		NICS (ppm)	-13.47	-2.41	-12.47	-13.97
<b>Me<sub>3</sub>POR</b>	$\Delta H$ 46.2	$E_R$ (kcal/mol)	0.0	+46.2	+42.8	+42.3
	$(\Delta G$ 48.6)	$\Delta H$ ( $\Delta G$ )	(0.0)	(+48.6)	(+44.8)	(+43.4)
		$\Phi_p$ (deg)	0.0	96.5	123.4	126.1
		NICS (ppm)	-14.29	-3.21	-12.31	-15.17

**TABLE 2: Energy Profiles, Rotational Angles, and NICS Values for the Rotation of Pyrrole Rings in the N-Confused Porphyrins**

	$E_A$ (kcal/mol)		NCP3H	NCP2H	NCP2Hts	NCP2Hinv	NCP3Hinv
<b>NCP</b>	$\Delta H$ 24.5	$E_R$ (kcal/mol)	0.0	+7.0	+31.5	+24.2	+21.6
	( $\Delta G$ 25.3)	$\Delta H$ ( $\Delta G$ )	(0.0)	(+6.9)	(+32.2)	(+24.7)	(+21.2)
		$\Phi_P$ (deg)	17.80	7.91	93.68	135.77	134.32
		NICS (ppm)	-13.76	-7.21	-2.39	-10.17	-14.60
<b>C<sub>6</sub>H<sub>5</sub>NCP</b>	$\Delta H$ 20.4	$E_R$ (kcal/mol)	0.0	+4.9	+25.3	+14.4	+12.2
	( $\Delta G$ 20.5)	$\Delta H$ ( $\Delta G$ )	(0.0)	(+5.3)	(+25.8)	(+14.7)	(+12.1)
		$\Phi_P$ (deg)	26.5	20.01	78.45	136.2	135.1
		NICS (ppm)	-11.90	-6.03	-1.38	-8.55	-12.49
<b>C<sub>6</sub>F<sub>5</sub>NCP</b>	$\Delta H$ 18.1	$E_R$ (kcal/mol)	0.0	+6.0	+24.1	+16.1	+16.1
	( $\Delta G$ 18.7)	$\Delta H$ ( $\Delta G$ )	(0.0)	(+5.5)	(+24.2)	(+16.0)	(+15.1)
		$\Phi_P$ (deg)	22.9	9.8	92.1	135.3	135.8
		NICS (ppm)	-12.15	-6.46	-2.12	-9.52	-13.39
<b>Me<sub>7</sub>NCP</b>	$\Delta H$ 23.1	$E_R$ (kcal/mol)	0.0	+7.9	+31.0	+25.1	+22.9
	( $\Delta G$ 24.5)	$\Delta H$ ( $\Delta G$ )	(0.0)	(+8.8)	(+33.3)	(+27.2)	(+23.6)
		$\Phi_P$ (deg)	18.2	8.7	93.5	130.3	131.9
		NICS (ppm)	-13.29	-6.96	-2.37	-8.79	-13.97

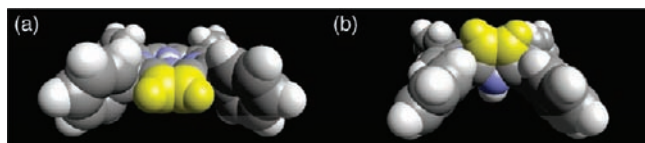
repulsion between the rotating pyrrole ring and the neighboring *meso*-phenyl groups. Whereas the moderate steric repulsion between the rotating pyrrole ring and the neighboring *meso*-phenyl groups is expected in the planar conformation, the less steric repulsion is found for the transition state as well as the inverted conformation on the basis of the space-filling models (Figure 13). This steric repulsion results in the destabilization of the planar conformation relative to the transition state and the inverted conformation. In the pentafluorophenyl derivative (**C<sub>6</sub>F<sub>5</sub>POR**), the lower activation energy barrier by 9 kcal/mol than the unsubstituted derivative was obtained. This value is similar to **C<sub>6</sub>H<sub>5</sub>POR**, which would suggest that the electronic perturbation at the *meso*-positions is less important. This is further supported by the calculation for **Me<sub>8</sub>POR**, where the relative energies of each conformer resemble those of **POR**. The possible electron donation from the methyl groups to the [18]annulenic skeleton would give almost no effect on the

activation energy barrier for the pyrrole rotation. The study on the N-confused porphyrin derivatives also leads to the important contribution of the steric repulsion and minor contribution of the electronic perturbation. Thus, the calculation on **Me<sub>7</sub>NCP** affords the similar energy profile to the calculation on **NCP**. The calculations on **C<sub>6</sub>H<sub>5</sub>NCP** and **C<sub>6</sub>F<sub>5</sub>NCP** give the activation energy barriers lower than **NCP** by 4 and 6 kcal/mol, respectively.

#### 4. Conclusion

The rotation of the pyrrole rings in the regular porphyrins and the N-confused porphyrins were studied with the DFT calculations. The activation energy barriers in the regular porphyrins are significantly large (36.5–49.1 kcal/mol), being consistent with the experimental observation. Meanwhile, the drastic decrease of the activation energy barriers is found in the N-confused porphyrin (18.1–24.5 kcal/mol). Although a 360° rotation of the pyrrole rings would be difficult possibly due to the small cavity of the macrocycles, the possible reaction pathway for production of N-fused porphyrin is obtained alternatively.

The factors to decrease the activation energy barriers by about 25 kcal/mol in the N-confused porphyrins could be explained as follows. (1) The transition state structures of the regular porphyrins and the N-confused porphyrins have the similar

**Figure 13.** Space-filling models of (a) **POR** and (b) **PORTs1**.



thermodynamic stability. When the confused pyrrole ring is nearly perpendicular to the rest of the tripyrrane unit, the effect of confusion is negated and almost no difference is observed between the regular and N-confused porphyrins. (2) In the initial planar conformations, the N-confused porphyrins are much less stable than the regular porphyrins due to the loss of the intramolecular hydrogen bondings inside the macrocycle, which would cause the lower activation energy barriers by 15–20 kcal/mol. (3) In the regular porphyrins, the rotation process is corresponding to the direct conversion from the strongly aromatic planar structure to the nonaromatic transition state structure and, thus, it would require the high activation energy barriers. Meanwhile, the partial loss of the aromatic stabilization energy is possible through the NH tautomerism prior to the pyrrole rotation in the N-confused porphyrins. This NH tautomerism would contribute to decrease the activation energy barriers by 5–10 kcal/mol. (4) Introduction of the  $\beta$ -alkyl substituents does not affect the activation energy barriers, while introduction of the *meso*-aryl groups contributes to decrease the activation energy barriers by 4–13 kcal/mol possibly due to the steric repulsion between the rotating pyrrole ring and the adjacent *meso*-aryl groups.

The information obtained here would be helpful for understanding molecular conformation and flexibility in porphyrin chemistry and also for a molecular design toward unique macrocyclic architectures, as well as a control of conformations in porphyrin-related macrocycles.

**Acknowledgment.** The present work was supported by the Grant-in-Aid for Scientific Research (19750036 and 21750047) and the Global COE Program “Science for Future Molecular Systems” from the Ministry of Education, Culture, Sports, Science and Technology of Japan.

**Supporting Information Available:** The tables of the Cartesian atom coordinates, the absolute energies of the optimized structures, and the results of the frequency calculations. This material is available free of charge via the Internet at <http://pubs.acs.org>.

## References and Notes

- (1) Kottas, G. S.; Clarke, L. I.; Horinek, D.; Michl, J. *Chem. Rev.* **2005**, *105*, 1281.
- (2) Pophristic, V.; Goodman, L. *Nature* **2001**, *411*, 565.
- (3) (a) Shimizu, S.; Osuka, A. *Eur. J. Inorg. Chem.* **2006**, 1319. (b) Srinivasan, A.; Furuta, H. *Acc. Chem. Res.* **2005**, *38*, 10. (c) Chandrashekar, T. K.; Venkatraman, S. *Acc. Chem. Res.* **2003**, *36*, 676.
- (4) (a) Suzuki, M.; Osuka, A. *J. Am. Chem. Soc.* **2007**, *129*, 464. (b) Toganoh, M.; Kimura, T.; Furuta, H. *Chem. Commun.* **2008**, 102. (c) Toganoh, M.; Kimura, T.; Furuta, H. *Chem.—Eur. J.* **2008**, *14*, 10585.
- (5) Pacholska, E.; Latos-Grażyński, L.; Ciniuk, Z. *Angew. Chem., Int. Ed.* **2001**, *40*, 4466.
- (6) Whereas huge numbers of examples about deformation from planar conformation have been reported, no one is significantly related to pyrrole rotation.
- (7) (a) Sprutta, N.; Latos-Grażyński, L. *Chem.—Eur. J.* **2001**, *7*, 5099. (b) Rath, H.; Sankar, J.; Prabhuraja, V.; Chandrashekar, T. K.; Joshi, B. S.; Roy, R. *Chem. Commun.* **2005**, 3343. (c) Setsune, J.; Mori, M.; Okawa, T.; Maeda, S.; Lintuluoto, J. M. *J. Organomet. Chem.* **2007**, *692*, 166. (d) Tanaka, Y.; Hoshino, W.; Shimizu, S.; Youfu, K.; Aratani, N.; Maruyama, N.; Fujita, S.; Osuka, A. *J. Am. Chem. Soc.* **2004**, *126*, 3046.
- (8) (a) Furuta, H.; Asano, T.; Ogawa, T. *J. Am. Chem. Soc.* **1994**, *116*, 767. (b) Chmielewski, P. J.; Latos-Grażyński, L.; Rachlewicz, K.; Głowiak, T. *Angew. Chem., Int. Ed. Engl.* **1994**, *33*, 779. (c) Morimoto, T.; Taniguchi, S.; Osuka, A.; Furuta, H. *Eur. J. Org. Chem.* **2005**, 3887.
- (9) (a) Furuta, H.; Ishizuka, T.; Osuka, A.; Ogawa, T. *J. Am. Chem. Soc.* **1999**, *121*, 2945. (b) Furuta, H.; Ishizuka, T.; Osuka, A.; Ogawa, T. *J. Am. Chem. Soc.* **2000**, *122*, 5748. (c) Ishizuka, T.; Ikeda, S.; Toganoh, M.; Yoshida, I.; Ishikawa, Y.; Osuka, A.; Furuta, H. *Tetrahedron* **2008**, *64*, 4037.
- (10) (a) Toganoh, M.; Ishizuka, T.; Furuta, H. *Chem. Commun.* **2004**, 2464. (b) Toganoh, M.; Ikeda, S.; Furuta, H. *Inorg. Chem.* **2007**, *46*, 10003. (c) Młodzianowska, A.; Latos-Grażyński, L.; Sztrenberg, L.; Stępień, M. *Inorg. Chem.* **2007**, *46*, 6950. (d) Młodzianowska, A.; Latos-Grażyński, L.; Sztrenberg, L. *Inorg. Chem.* **2008**, *47*, 6364.
- (11) (a) Toganoh, M.; Kimura, T.; Uno, H.; Furuta, H. *Angew. Chem., Int. Ed.* **2008**, *47*, 8913. (b) Gupta, I.; Srinivasan, A.; Morimoto, T.; Toganoh, M.; Furuta, H. *Angew. Chem., Int. Ed.* **2008**, *47*, 4563.
- (12) Ishizuka, T.; Osuka, A.; Furuta, H. *Angew. Chem., Int. Ed.* **2004**, *43*, 5077.
- (13) Toganoh, M.; Konagawa, J.; Furuta, H. *Inorg. Chem.* **2006**, *45*, 3852.
- (14) (a) Sztrenberg, L.; Latos-Grażyński, L. *J. Porphyrins Phthalocyanines* **2001**, *5*, 474. (b) Furuta, H.; Maeda, H.; Osuka, A. *J. Org. Chem.* **2000**, *65*, 4222. (c) Furuta, H.; Maeda, H.; Osuka, A. *J. Org. Chem.* **2001**, *66*, 8563. (d) Vyas, S.; Hadad, C. M.; Modarelli, D. A. *J. Phys. Chem. A* **2008**, *112*, 6533. (e) Ghosh, A. *Angew. Chem., Int. Ed. Engl.* **1995**, *34*, 1028. (f) Kiran, B.; Nguyen, M. T. *J. Organomet. Chem.* **2002**, *643–644*, 265.
- (15) Furuta, H.; Ishizuka, T.; Osuka, A.; Dejima, H.; Nakagawa, H.; Ishikawa, Y. *J. Am. Chem. Soc.* **2001**, *123*, 6207.
- (16) (a) Hohenberg, P.; Kohn, W. *Phys. Rev.* **1964**, *136*, B864. (b) Kohn, W.; Sham, L. J. *Phys. Rev.* **1965**, *140*, A1133.
- (17) Frisch, M. J.; Trucks, G. W.; Schlegel, H. B.; Scuseria, G. E.; Robb, M. A.; Cheeseman, J. R.; Montgomery, J. A., Jr.; Vreven, T.; Kudin, K. N.; Burant, J. C.; Millam, J. M.; Iyengar, S. S.; Tomasi, J.; Barone, V.; Mennucci, B.; Cossi, M.; Scalmani, G.; Rega, N.; Petersson, G. A.; Nakatsuji, H.; Hada, M.; Ehara, M.; Toyota, K.; Fukuda, R.; Hasegawa, J.; Ishida, M.; Nakajima, T.; Honda, Y.; Kitao, O.; Nakai, H.; Klene, M.; Li, X.; Knox, J. E.; Hratchian, H. P.; Cross, J. B.; Adamo, C.; Jaramillo, J.; Gomperts, R.; Stratmann, R. E.; Yazyev, O.; Austin, A. J.; Cammi, R.; Pomelli, C.; Ochterski, J. W.; Ayala, P. Y.; Morokuma, K.; Voth, G. A.; Salvador, P.; Dannenberg, J. J.; Zakrzewski, V. G.; Dapprich, S.; Daniels, A. D.; Strain, M. C.; Farkas, O.; Malick, D. K.; Rabuck, A. D.; Raghavachari, K.; Foresman, J. B.; Ortiz, J. V.; Cui, Q.; Baboul, A. G.; Clifford, S.; Cioslowski, J.; Stefanov, B. B.; Liu, G.; Liashenko, A.; Piskorz, P.; Komaromi, I.; Martin, R. L.; Fox, D. J.; Keith, T.; Al-Laham, M. A.; Peng, C. Y.; Nanayakkara, A.; Challacombe, M.; Gill, P. M. W.; Johnson, B.; Chen, W.; Wong, M. W.; Gonzalez, C.; Pople, J. A. *Gaussian 03, Revision C.02*, Gaussian, Inc., Wallingford CT, 2004.
- (18) (a) Becke, A. D. *J. Phys. Chem.* **1993**, *98*, 5648. (b) Lee, C.; Yang, W.; Parr, R. G. *Phys. Rev. B* **1988**, *37*, 785. (c) Vosko, S. H.; Wilk, L.; Nusair, M. *Can. J. Phys.* **1980**, *58*, 1200. (d) Stephens, P. J.; Devlin, F. J.; Chabalowski, C. F.; Frisch, M. J. *J. Phys. Chem.* **1994**, *98*, 11623.
- (19) Schleyer, P. v. R.; Maerker, C.; Dransfeld, A.; Jiao, H.; van Eikema Hommes, N. J. R. *J. Am. Chem. Soc.* **1996**, *118*, 6317.
- (20) Kohn-Sham orbitals of **PORinv2** are also essentially same with those of **POR**.
- (21) Relationship between aromaticity and a number of  $\pi$ -electrons is reversed from standard conformation in Möbius conformation:  $[4n+2]\pi$  Hückel, aromatic;  $[4n+2]\pi$  Möbius, antiaromatic;  $4n\pi$  Hückel, antiaromatic;  $4n\pi$  Möbius, aromatic.
- (22) (a) Herges, R. *Chem. Rev.* **2006**, *106*, 4820. (b) Kawase, T.; Oda, M. *Angew. Chem., Int. Ed.* **2004**, *43*, 4396.
- (23) (a) Ajami, D.; Oeckler, O.; Simon, A.; Herges, R. *Nature* **2003**, *426*, 819. (b) Stępień, M.; Latos-Grażyński, L.; Sprutta, N.; Chwalisz, P.; Sztrenberg, L. *Angew. Chem., Int. Ed.* **2007**, *46*, 7869. (c) Tanaka, Y.; Saito, S.; Mori, S.; Aratani, N.; Shinokubo, H.; Shibata, N.; Higuchi, Y.; Yoon, Z. S.; Kim, K. S.; Noh, S. B.; Park, J. K.; Kim, D.; Osuka, A. *Angew. Chem., Int. Ed.* **2008**, *47*, 681.
- (24) Halogenation is so far essential for formation of N-fused porphyrin from N-confused porphyrin without assistance of other reagents.